



Article

# Development and Identification of Working Parameters for a Lychee Peeling Machine Combining Rollers and a Pressing Belt

Lu Minh Le <sup>1,\*</sup>, Thong Chung Nguyen <sup>1</sup>, Binh Thai Pham <sup>2</sup>, Hai-Bang Ly <sup>2</sup> , Vuong Minh Le <sup>1</sup> and Tien-Thanh Le <sup>3,\*</sup>

<sup>1</sup> Faculty of Engineering, Vietnam National University of Agriculture, Hanoi 100000, Vietnam; ncthong@vnua.edu.vn (T.C.N.); vuongminhle09@gmail.com (V.M.L.)

<sup>2</sup> University of Transport Technology, Hanoi 100000, Vietnam; binhpt@utt.edu.vn (B.T.P.); banglh@utt.edu.vn (H.-B.L.)

<sup>3</sup> Institute of Research and Development, Duy Tan University, Da Nang 550000, Vietnam

\* Correspondence: lmlu@vnua.edu.vn (L.M.L.); letienthinh@duytan.edu.vn (T.T.L.); Tel.: +84-24-6261-7699 (L.M.L. & T.T.L.)

Received: 21 October 2019; Accepted: 15 November 2019; Published: 18 November 2019



**Abstract:** This work describes the development, design, and parameter identification of a lychee peeling machine. The working principle of the machine combines two rollers with a pressing belt to separate the peel from the fruits. It was designed and its operational parameters identified on the basis of experimental data on the Thieu lychee, which currently covers about 80% of the plantation area in Vietnam. To this end, the first step was to measure the physical characteristics of the fruits, such as size, shape, and density. Moreover, the coefficient of static friction between lychees and rubber rollers, and the critical peeling force, were identified, with a view to optimizing the operational parameters later on. Results showed that a minimum tangential force of 10.5 N is needed to break the peel and separate it from the pulp. Based on the balanced force principle, various optimal machine parameters such as roller rotation speed, roller diameter, roller length, gap size between the two rollers, belt velocity, and minimum pressure of the belt were calibrated. In addition, spiral grooves were created on the roller surface to facilitate the motion of the fruits. The optimal results were roller size 900 × 100 mm (length × diameter), rotation speed 159 RPM, gap size between rollers 4 mm, belt size 850 × 60 mm (length × width), belt pressure 13.5 N, and belt velocity 140 mm/s. Using the design and operational parameters mentioned above, the machine was able to perform regularly at a throughput of 100 kg/h, as demanded by the current market. Moreover, it would be easily feasible to combine multiple pairs of rollers and pressing belts in order to increase throughput. The methodology for the design of this peeling machine and identification of working parameters with respect to experimental data could be applied in many other post-harvesting configurations.

**Keywords:** lychee; peeling machine; friction; machine operational parameters; peeling principle

## 1. Introduction

The lychee is a tropical fruit tree, growing mainly in the northern provinces of Vietnam and in many other countries such as China, India, and South Africa [1–3]. This fruit tree has particularly high economic value in Vietnam [4,5]. The Vietnamese lychee plantation currently covers an estimated 30,000 hectares, with an agricultural output of 150,000 tons per year, and it is continually increasing [4]. Lychee products which are particularly successful on the world market include fresh and processed fruits (e.g., dried and canned lychees, juice, or liqueur [1,6–8]). In recent years, Vietnamese fresh and canned lychee fruits have been consumed in huge quantities in various international markets,

including France, Germany, the Netherlands, Switzerland, South Korea, Malaysia, Australia, Japan, and China [4,9].

However, due to the short harvesting window, manufacturers of lychee products often have to hire seasonal workers in large numbers to manually process the fruits at various stages, such as harvesting, peeling, and separating seeds [4,5,10]. Even so, the crop yield remains low, and it is impossible to be assured of meeting market demand [4,11]. Moreover, when such supply chains are used for manufacturing processed lychee fruits, both food hygiene and product quality might be insufficient [12,13]. Therefore, there is an urgent need to develop a mechanical automatic lychee peeling machine to replace high-risk manual labor, particularly in a developing country like Vietnam. Moreover, given that the plantation area is growing continuously, such mechanization could bring real benefits.

There are many technologies that are applied to the peeling of tubers and fruits—for instance, based on the principles of impact, friction, or shearing [14,15] or using infrared radiation heating [16]. In the case of the principle of impact, the peeling force is generated by moving fruits repeatedly hitting hard surfaces [14,17,18], so that the shell cracks and separates from the flesh. However, this principle is only suitable for fruits and tubers with hard peel. With the friction principle, the peeling force is the friction generated by compressive pressure between a working part of the machine and fruits, or between fruits and other fruits [14]. Machines based on this principle tend to be designed using two discs or rollers, rotating at a differential speed. This type of machine exhibits high peeling performance but low yield and high breakage rate. Moreover, the friction generates heat, meaning that the fruits can easily become partially cooked, which is undesirable. In the case of the shearing principle, peeling force is created by pressing and shearing—for instance, using rubber-covered rollers [19]. As the rollers rotate, the fruit is compressed, and shear causes the peel to crack and separate from the pulp.

Based on the peeling principles mentioned above, various mechanization systems have been introduced in prior literature to improve peeling efficiency for several types of fruits, including citrus [20], mandarin [21], tomato [22], and cassava [23]. Chen et al. [20] proposed a citrus peeling machine based on a scissor cutting system. In this work, typical mechanical properties of citrus fruits, such as maximum tensile force and displacement in the separation of peel, were measured to serve as indicators in designing the machine. In another attempt, Jimoh et al. [23] made improvements to their previous cassava peeling tool by using the impact principle. The machine's operational parameters were determined when working with different varieties of cassava involving throughput capacity, peeling efficiency, peel retention, mechanical damage, and quality performance efficiency. Pan et al. [21] developed a roller-based mandarin peeling machine involving three consecutive stages of processing—gear tooth peeling rollers, arc gear tooth peeling rollers, and residual peel removal. This machine's mandarin peeling efficiency was at least 97.5%, while the damage rate was lower than 2.68%. Thus far, mechanization systems for fruit peeling could greatly increase throughput as well as saving time and labor-intensity.

In terms of a lychee peeling machine, several efforts have been conducted to develop an automatic lychee peeler in China and India. The ICAR-Central Institute of Post-Harvest Engineering & Technology (CIPHET), Ludhiana, Punjab, India, has introduced a lychee peeler based on the principle of friction and piercing, which consists of two rollers rotating at differential speed in opposite directions [24,25]. One roller has a knurled surface, while the other has spikes. Due to rotational movement, the spike makes a cut on the peel (i.e., it pierces the peel of fruit as the fruit touches the spikes), whereas the other cylinder restricts the motion of the fruit because of friction with the knurling surface. Such a design allows the fruits to be quickly peeled through the open cut. However, if the dimension of the spikes is not properly selected, a significant amount of flesh could be damaged. Moreover, the probability of breakage just after peeling is relevant when other spikes come to make cuts on the fruit due to circular motion of the roller. In addition, the capacity of the equipment has been shown to be up to 50–80 kg/h, with an optimal peeling efficiency of 96%. In China, various lychee peeling systems have also been developed and patented [26]. For instance, Henan Hiwant International

Co., Ltd, has been a Chinese innovative and professional company in the research, development, manufacture, and marketing of fruit processing machines. They have developed and commercialized a series of friction-based peeling machine for lychee (longan and rambutan), including LX-1A, LX-2A, and LX-3A models [27]. Their machines, mainly composed of a couple of rollers, exhibit a remarkable peeling rate, which is over 99%, and pulp loss rate is less than 1%. Such machines could work with a maximum throughput of 2–3 tones/h (model LX-3A). However, the cost is extremely high (i.e., more than 25,000 USD per unit). Nevertheless, it is noteworthy to mention that such machines are ideal for massive industrial production.

There remains a number of drawbacks to a lychee peeling machine based on pure friction—high rate of breakage, flesh damage, and loss of pulp. The main reason is that fruits jump within the machine, owing to insufficient compression. Thus, an appropriate machine combining friction and shearing principles for the peeling of lychees was developed in the Faculty of Engineering, Vietnam National University of Agriculture. This machine was able to peel the lychees with a high rate of throughput and without affecting the fruit pulp. Moreover, to the best of the authors' knowledge, a hybrid technique such as this has not yet been addressed. Besides, in order to establish the relation between the Vietnamese lychee crop and the machine's operational parameters, it has hitherto been crucial to design the machine on the basis of experimental data. Finally, such a self-developed mechanization system could help more and more Vietnamese manufacturers of lychee products to increase their yield.

To this end, the physical characteristics, composition, and mechanical properties of fresh lychee fruits were first determined experimentally. The data were then used to inform the design of the hybrid friction-shearing peeling machine. Finally, the machine's operational parameters were identified on the basis of experimental data. This investigation favors agricultural mechanization, as the move greatly increases farm productivity.

## 2. Materials and Methods

### 2.1. Lychee Fruits and Their Physical Characteristics

Common Vietnamese lychee varieties are now divided into three groups—early, medium, and late ripening [28]. In particular, the predominant lychee variety is late ripening, which covers about 80% of the plantations in Vietnam [5]. This variety, called Thieu (see Figure 1), yields the smallest fruit of all current lychee varieties. Thieu lychee fruits are usually circular, oval, or heart-shaped, surrounded by a thin, tough, rough, but soft crust, so they are easy to peel if they are still fresh [29]. Three hundred significant Thieu lychee fruits were randomly selected from 10 kg (approximately 500 fruits) for experimental measuring of dimensions and weight. In our study, the dimensions of the fruits were measured using a vernier caliper with a resolution of 0.02 mm, whereas their weight was measured using Mettler Toledo MS1602S (Mettler Toledo, LLC, Columbus, OH, USA) electronic scale, which exhibits a resolution of 0.02 g and a maximum capacity of 1620 g (see Figure 2).

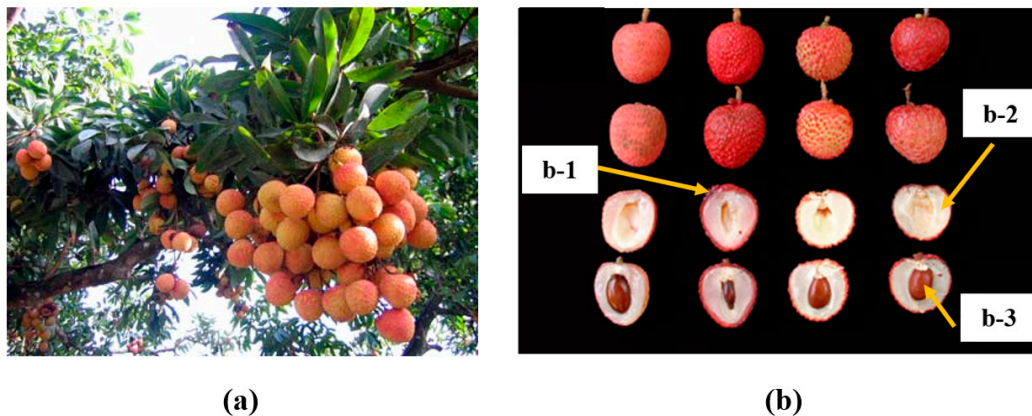


**Figure 1.** Visualisation of lychee fruits: (a) clusters and (b) composition of lychee fruit: (b-1) peel; (b-2) flesh, and (b-3) seed.



**Figure 2.** Mettler Toledo MS1602S electronic scale used in this study.

## 2.2. Experiments Testing Lychees' Mechanical Friction Properties

In order to design a suitable fruit processing machine, it is essential to determine the fruit's mechanical properties. The existing literature reveals numerous investigations to characterize the mechanical properties of fresh fruits, including longan [30], watermelon [31], potato [32], kiwi [33,34], and orange [35]. In terms of lychee fruits, Chen et al. [36,37] conducted both compression and tensile tests to determine the elastic modulus, rupture force, failure energy, stiffness, and failure strength of fresh lychee fruits and their stones. They found that the peel's elastic modulus in the horizontal direction was greater than that in the vertical direction. They also suggested a further study, investigating the interaction between lychee fruits, their stone and peel in terms of effective mechanical properties. Based on the results of these experiments, a mechanical model of lychee fruits was subsequently put forward by Chen et al. [38] using the numerical finite element method. This model was helpful in providing basic information for the design of processing equipment. For instance, the clamping and cutting devices in a lychee harvesting robot were designed and tested in Chen et al. [39]. In another work, Wang et al. [40] reported the mechanical damage to lychee fruits caused by fruit-on-fruit impact. The two lychee varieties investigated were Yuhebao and Guiwei, grown mainly near Guangzhou, China. Xiong et al. [41] used hyperspectral imaging to detect micro-damage in lychees. This technique was useful in quantifying the influence of various stages such as harvesting, preservation, storage, and transportation on lychee fruit damage [42].

In this paper, the Vietnamese Thieu variety of lychee was used for the mechanical tests. All tests were conducted at the Strength of Materials Laboratory, Faculty of Engineering, Vietnam National

University of Agriculture. Figure 3 is a diagram of the experimental setup to determine critical peeling force using the friction-shearing principle.

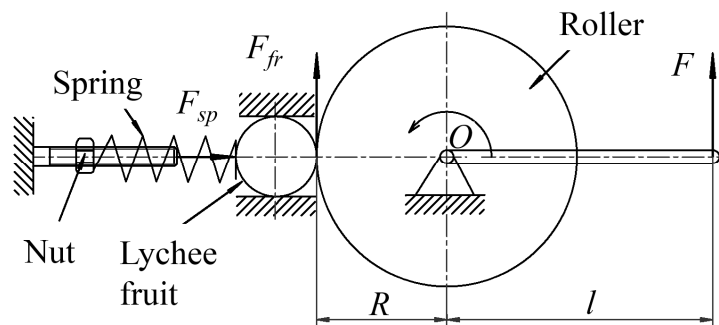


Figure 3. Diagram of experimental setup to determine critical peeling force.

In this setup, a lychee is tightly pressed by a spring of a given stiffness  $k$  into a rubber-covered roller. This compressive force can be determined by the deformed length  $\lambda$  of the spring and can be adjusted by means of a nut at the top end of the spring. The roller of radius  $R$  is fitted with a lever arm  $l$ . On the top end of the lever arm, a dynamometer measures the force  $F$  exerted on the arm. When we tighten the nut, the spring will apply a force  $F_{sp}$  to the fruit,

$$F_{sp} = k\lambda \tag{1}$$

The lychee is also subjected to pressure  $N = F_{sp}$  by the roller. Because the lever arm is rigidly connected to the roller, at the point of contact between the roller and the fruit, a friction force, denoted by  $F_{fr}$ , occurs against the torque. If this friction force reaches a critical value, the peel begins to separate from the fruit. The friction force can be determined by the following equation:

$$F_{fr} = \frac{F \times l}{R} \tag{2}$$

Therefore, by progressively increasing the force exerted on the spring (tightening the nut) and force exerted on the lever arm (force  $F$ ), critical peeling force can be achieved. At the same time, the coefficient of static friction between the fruits and the rubber is measured by the GuntTM22 (G.U.N.T. Gerätebau GmbH, Barsbüttel, Germany) measuring device (see Figure 4) at the Strength of Materials Laboratory, Faculty of Engineering. Lychees are set on a 5 mm rubber-covered plate. The plate is inclined gradually until the fruits begin to slide down. The corresponding tilt angle of the plate was then recorded to deduce the coefficient of static friction between the lychee fruits and the plate (as the tangent of the tilt angle [43–45]). In addition, the measurement was replicated 20 times.

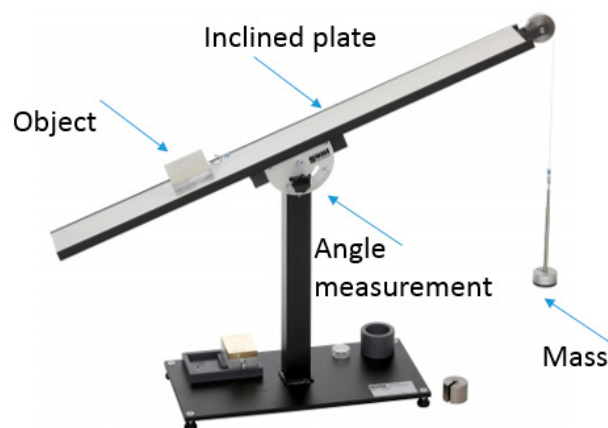
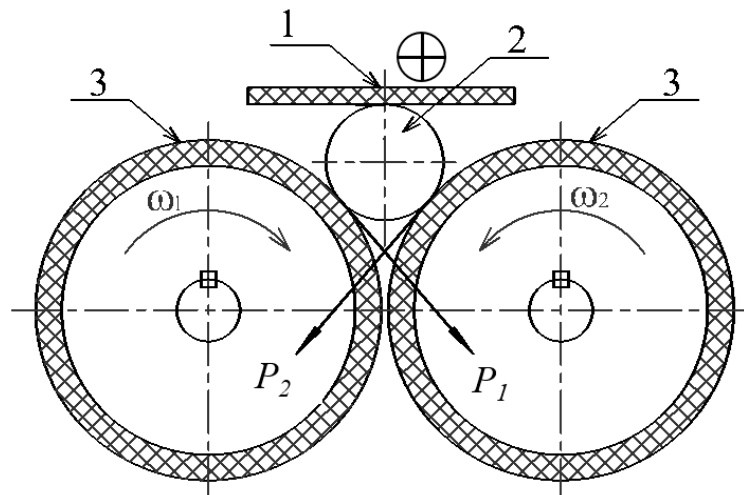


Figure 4. GuntTM22 device for measuring coefficient of friction.

### 2.3. Description of Peeling Working Principle

The peeling part of machine consists of two rubber-covered rollers and a pressing belt on top of the rollers, as shown in Figure 5. The belt is parallel to the plane formed by the two axes of the cylinders. Based on the peeling friction principle, the two rollers rotate in opposite directions, whereas the belt exhibits a translation movement along the axial direction of the rollers. This motion and the location of the belt forced the lychee fruits to move along the rollers in the axial direction, preventing fruit from jumping and suffering serious damage. As the belt moves, the lychee is pressed into the rollers. The peel is then easily separated from the pulp by the combination of friction and shearing forces between the fruit, rollers, and belt.



**Figure 5.** Diagram of the peeling part of the machine—(1) pressing belt; (2) lychee fruit; (3) rollers.

### 2.4. Description of the Whole Machine

Figure 6 shows a diagram of the developed peeling machine. The machine operates on the following principle. After sorting, washing and drying, lychees are put on the conveyor (1). The conveyor transfers the fruits to the gutter (2), which directs them in a row. Next, the peel is slightly cut by a blade (3), to provisionally break the lychee peel and weaken it. The fruits then fall into the peeling part, consisting of two rubber-covered rollers (4) and the pressing belt (8), as detailed in Section 2.3. The rollers and belt are inclined at an angle  $\alpha$  with respect to the horizontal. Spiral grooves (10) are created on the roller surface for obtaining an appropriate friction between the rollers and the fruit (i.e., guide the fruit move forward along the axial direction of the roller). The velocity of the compression belt is set in accordance with the peeling capacity of the rollers. The peel and juice both fall into the collection bin (5), where they are retrieved separately by screw (6) and machine part (7), respectively. Finally, the peeled lychee fruit goes down the conveyor (9) to the next stage of processing. To increase the ability to peel the fruit, the rollers are more densely grooved at the beginning. On the other hand, to avoid crushing the fruits, the end of the rollers is smoother, and the end of the belt is adjusted, shifting away from the rollers to reduce the pressure on the fruit.

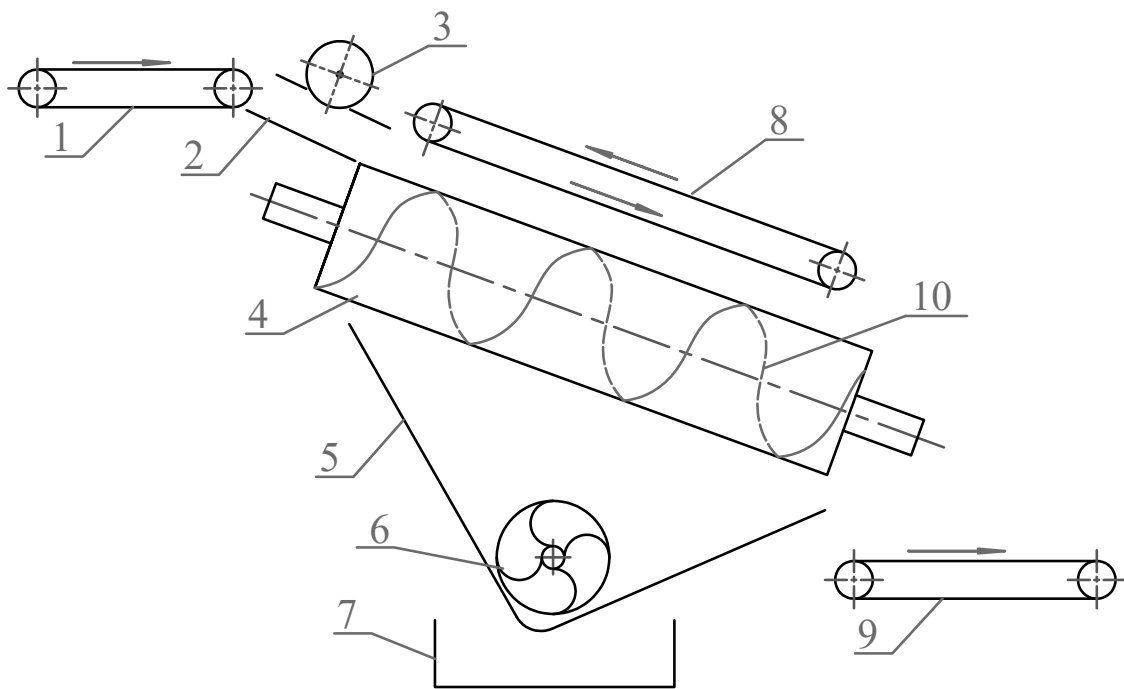


**Figure 6.** Diagram of the peeling machine—(1) sorting conveyor; (2) gutter, (3) blade; (4) rubber-covered roller; (5) collection bin; (6) screw; (7) machine part for collecting juice; (8) pressing belt; (9) conveyor of peeled fruits; (10) spiral groove on the roller surface.

### 2.5. Flowchart Methodology

The flowchart methodology of this study is presented in Figure 7, consisting of the following four main steps:

- **Step I:** Selection of working principle. In this step, the chosen working principle combining friction and shearing is detailed.
- **Step II:** Design of main machine parts, such as rollers, belt, and spiral grooved roller surface. Other parts of the machine were also indicated.
- **Step III:** The physical characteristics of lychee fruits and their mechanical properties—especially critical peeling force—were determined using equipment at the Strength of Materials Laboratory, Faculty of Engineering, Vietnam National University of Agriculture.
- **Step IV:** Analytical identification of working parameters. In this final step, the characteristics of the rollers, such as length, diameter, and gap as well as rotation speed; the characteristics of belt, such as length and width, velocity, and required pressure; and the characteristics of spiral groove, such as number, pitch, and depth, were calibrated based on earlier experimental data and the balanced force principle. Numerical simulation using Autocad Inventor, version 22.0 (Autodesk, San Rafael, CA, USA) was also performed for assembling of (moving and fixed) parts and fabrication of machine, for the use of experimental validation tests later.

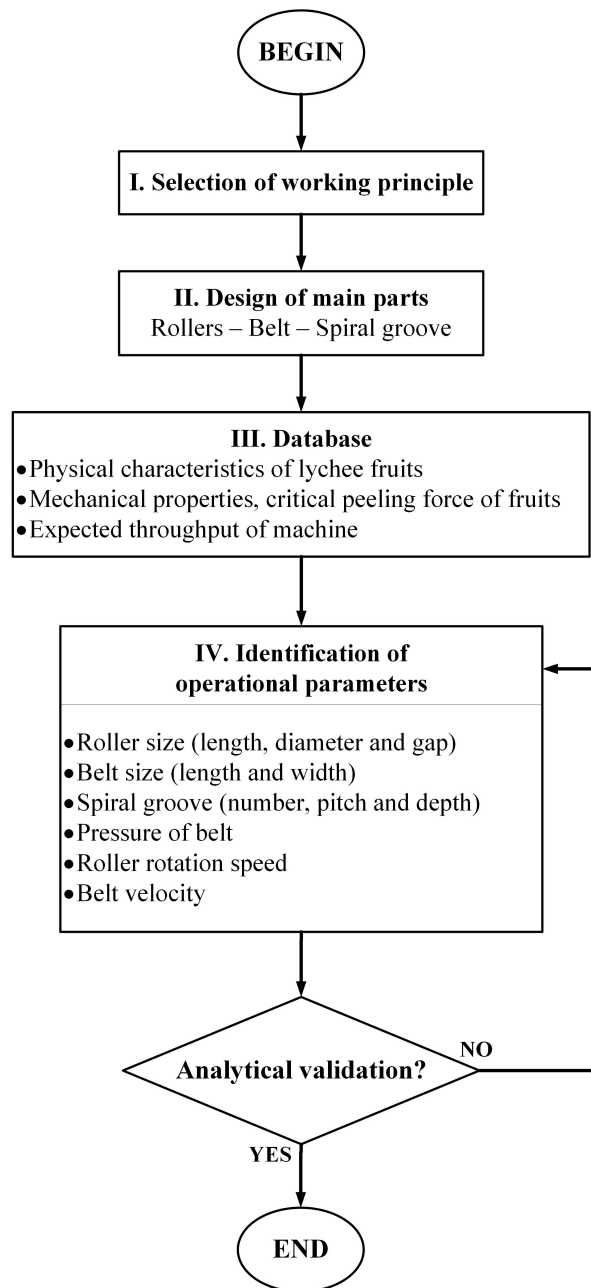


Figure 7. Flowchart methodology of the present study.

### 3. Results and Discussions

#### 3.1. Physical and Mechanical Properties of Lychee Fruits

##### 3.1.1. Physical Properties

The shape of Thieu lychees is slightly round; their length is 3.3–3.4 cm approximately, their average diameter is 3.4–3.5 cm approximately, length-to-diameter ratio is roughly 0.94–0.98, and average weight is approximately 20 g (see also Figure 1).

##### 3.1.2. Critical Peeling Force for Lychee Fruits

Using the experimental setup introduced in Section 2.2, the average critical peeling force was obtained as  $F_{cr} = 10.5$  N. Thus, in order to be able to peel lychees, it is necessary to apply a tangential

friction force equal to or greater than 10.5 N. In addition, the raised plate experiment showed that lychee fruits and rubber have a friction tilt angle of about 40–42°, meaning a coefficient of static friction of 0.90 can be deduced. These measurements were used later on to identify the operational parameters of the machine.

### 3.2. Analytical Identification of Machine Operational Parameters

Based on the current market demand, the expected average throughput of a pair of peeling rollers is 100 kg/h. The machine was designed to peel lychees ranging from 25 to 40 mm in diameter. The following are the operational parameters associated with the expected throughput.

#### 3.2.1. Identification of Optimal Roller Diameter, Gap Size, and Belt Pressure

When the fruit is in equilibrium position (the two rollers and the belt are standing as shown in Figure 8), the forces acting on the lychee include weight  $Q$  of the fruit, pressure  $H$  of the belt, and two reaction forces— $N_1, N_2$ —of the two rollers applied to the fruit, respectively. As the system shown is balanced, it can be deduced that

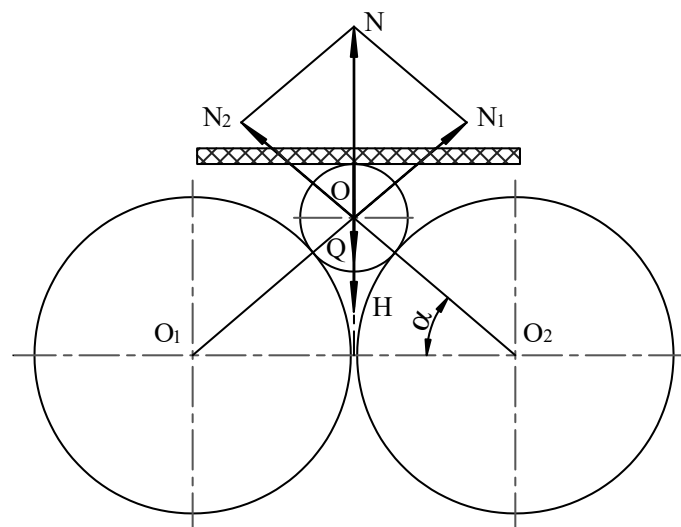


Figure 8. Diagram of forces exerted on the fruit when rollers are at rest.

$$Q + H = N \tag{3}$$

Assuming that the fruit is spherical, and the two rollers have the same diameter, the two forces  $N_1$  and  $N_2$  are equal,

$$N = 2N_1 \sin(\alpha), \tag{4}$$

where  $\alpha$  is the angle between the reaction force  $N_1$  or  $N_2$  and the horizontal. The reaction force is calculated using the following equation:

$$N_1 \approx N_2 = \frac{Q + H}{2 \sin(\alpha)} \tag{5}$$

When the rollers and belt start to move, as shown in Figure 9, the forces acting on the fruit include weight  $Q$  of the fruit, pressure  $H$  and friction force  $F_{fb}$  of the belt, and the forces of the two rollers applied to the fruit, respectively. There are two components of this force exerted by each roller—radial and tangential, denoted by  $N_1, N_2$  and  $P_1, P_2$ , respectively. The tangential part exists in this case due to the pressure between the fruit and the roller, consisting of the weight  $Q$  of the fruit plus the pressure  $H$  from the belt. Such tangential force is equal to the friction force between the fruit and the roller at the

point of contact. When the fruit starts to rotate, these forces create moments in opposite directions, breaking the peel strength. Note that hypotheses are made, including that the fruit is spherical, and that the two rollers have the same diameter and rotation speed. Using these hypotheses,

$$\begin{cases} P_1 = F_{fr1} = N_1 \times f \\ P_2 = F_{fr2} = N_2 \times f \\ P_1 \approx P_2 \end{cases} \quad (6)$$

where  $f$  is the friction coefficient between the fruit and the roller. As we see, the condition to peel the fruit is that the tangential force must be equal or greater than the critical peeling force  $F_{cr}$  determined in Section 3.1.2 (see Section 2.2 for the details of the experiments).

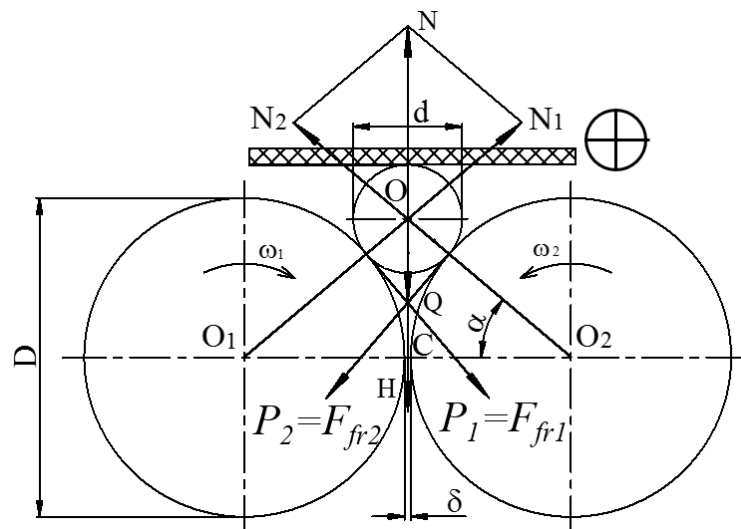


Figure 9. Diagram of forces exerted on the fruit when rollers are rotating.

$$P_1 = N_1 f \geq F_{cr} \quad (7)$$

In combining Equations (5)–(7), we deduce

$$\frac{Q + H}{2 \sin(\alpha)} f \geq F_{cr} \quad (8)$$

A condition for pressure H of the belt could be identified as

$$H \geq \frac{2F_{cr} \sin(\alpha)}{f} - Q \quad (9)$$

The relationship between the angle  $\alpha$  and the diameter of the rollers and fruit, as well as the gap between the two rollers can be determined by considering the triangle  $O_1OC$  as follows:

$$\cos(\alpha) = \frac{O_1C}{OO_1} = \frac{\frac{D+\delta}{2}}{\frac{D+d}{2}} = \frac{D+\delta}{D+d'} \quad (10)$$

where  $D$  is the roller diameter, in mm, and  $\delta$  is the gap between the two rollers, in mm.

The roller diameter and the gap between two rollers have a significant influence on the quality and capacity of the machine. On the one hand, if the roller diameter and the gap between the two rollers increase, the angle  $\alpha$  will decrease (see Figure 10a). Therefore, the required pressure  $H$  on the fruit will also increase, as shown by Equation (9), so the fruit will go deeper into the gap between the two rollers. This configuration is not optimal, because of loss of juice, pulp, and even small fruits may

become caught in the gap. Moreover, the design of the belt location is difficult because it may touch the rollers.

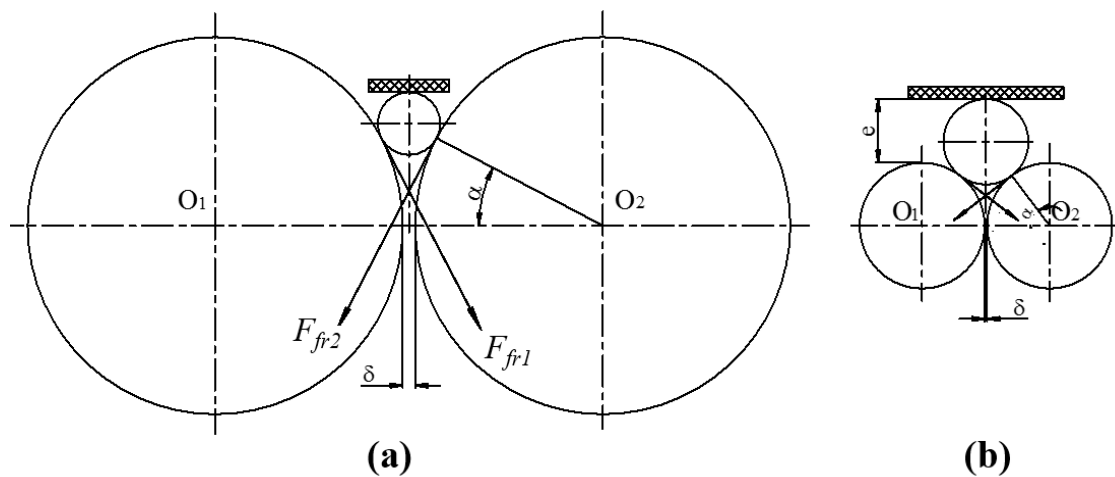


**Figure 10.** Diagram illustrating the influence of roller diameter and gap size. (a) When roller diameter and gap size are large; (b) When roller diameter and gap size are small.

On the other hand, if the diameter of the two rollers is small, the required pressure will also be small, but the two contact points between the fruit and the two rollers will be close to one another (see Figure 10b). For that reason, the deformation on the fruit skin (arc length between the two contact points) will also be small and not enough to stretch the peel and overcome its tensile strength. At the same time, the gap between the belt and the rollers grows, so that some fruits jump, and small fruits can fall through the gap between the belt and the rollers. Moreover, if the gap  $\delta$  between the two rollers is too small, the peel will not be able to pass through and can cause a blockage.

Therefore, the required roller diameter and gap between the rollers need to be calculated and selected carefully. The optimal diameter of the rollers should satisfy the following two conditions: (i) large enough to create frictional torque to peel the fruit and (ii) small enough to prevent the fruit passing through the gap between the two rollers. Similarly, the optimal gap should be (i) large enough to let the peel pass through without jamming and (ii) suitable to separate the peel from the pulp.

Analytical identification showed that the optimal roller diameter is in the range of 90–110 mm while the optimal gap size is in the range of 2–5 mm. In this study, we have chosen the following optimal parameters:  $D_{opt} = 100$  mm and  $\delta_{opt} = 4$  mm. Thus, the angle  $\alpha$  will fluctuate between  $33^\circ$  and  $42^\circ$  depending on the fruit size, while the minimum pressure  $H$  due to the belt is 13.5 N.

### 3.2.2. Identification of Roller Rotation Speed and Belt Velocity

The velocities of the belt and rollers determine the throughput of the machine. Assuming a lychee fruit is transported by the belt with pure rolling motion without sliding, so to ensure the expected throughput of  $q = 100$  kg/h, the velocity of the fruit (in mm/s) is determined to be

$$V_{fruit} = \frac{qZ_{fruit}a}{3600} = \frac{qZ_{fruit}\beta d}{3600}, \tag{11}$$

and the velocity of the belt (in mm/s) is calculated as

$$V_b = 2\gamma V_{fruit}, \tag{12}$$

where  $q$  is the expected throughput of a pair of rollers,  $Z_{fruit}$  is the average number of fruits weighing 1 kg,  $a$  is the distance between two consecutive fruits along the roller axis,  $d$  is the average diameter of

lychee fruits,  $\beta$  is the coefficient of distance between two consecutive fruits,  $V_b$  is the velocity of the belt, and  $\gamma$  is the coefficient of sliding of fruits.

In order to increase the friction between the rollers and the fruit and help the fruit move forward along the roller axis, spiral grooves are created on the roller surface. Additionally, the roller axial length should be sufficient to allow time for peeling. In this study, we have selected 16 spiral grooves, with a pitch of  $S = 22$  mm and the depth of the groove 1 mm. To facilitate the motion of the fruit on the roller surface, we have chosen the velocity of the spiral  $V_{spr}$  as equal to the velocity of the fruit. Based on this hypothesis, the roller rotation speed (in RPM) is determined as follows:

$$\omega_{roller} = \frac{60V_{spr}}{S} = \frac{60V_{fruit}}{S} \tag{13}$$

In order to completely peel one fruit, the minimum working length of the rollers should ensure that the fruit rolls on the roller surface for at least one round. However, other influencing factors such as the current location of the fruit along the roller axis and the preliminary cutting position on the peel should also be taken into account. Based on experimental tests, we have chosen the minimum number of rounds as  $n_r = 2.5$ . The minimum working length  $L_{wl}$  and the final length  $L_{opt}$  (in mm) of the rollers are calculated as

$$L_{wl} = \gamma\pi dn_r \tag{14}$$

$$L_{wl} + 300 \leq L_{opt} \leq L_{wl} + 350, \tag{15}$$

where the additional length between 300 and 350 mm was chosen in order to take into account the actual position of the fruit along the axial direction of the roller. Finally, Table 1 summarizes the optimal operational parameters of the developed lychee peeling machine for a given throughput of 100 kg/h. A 3D visualization of assembly of different parts using Autodesk Inventor [46] is shown in Figure 11. Such simulation allows us to (i) visualize the motion of moving parts and (ii) export engineering drawings for fabrication of machine, ready for experimental validation tests later.

**Table 1.** Optimal operational parameters of a machine for an expected throughput of 100 kg/h using a pair of rollers.

Number	Parameter	Optimal Value	SI Unit
1	Roller diameter	100	mm
2	Gap size between two rollers	4	mm
3	Roller length	900	mm
4	Roller rotation speed	159	RPM
5	Number of spiral grooves	16	-
6	Pitch of spiral groove	22	mm
7	Depth of spiral groove	1	mm
8	Belt length	850	mm
9	Belt width	60	mm
10	Belt speed	140	mm/s
11	Belt pressure	13.5	N

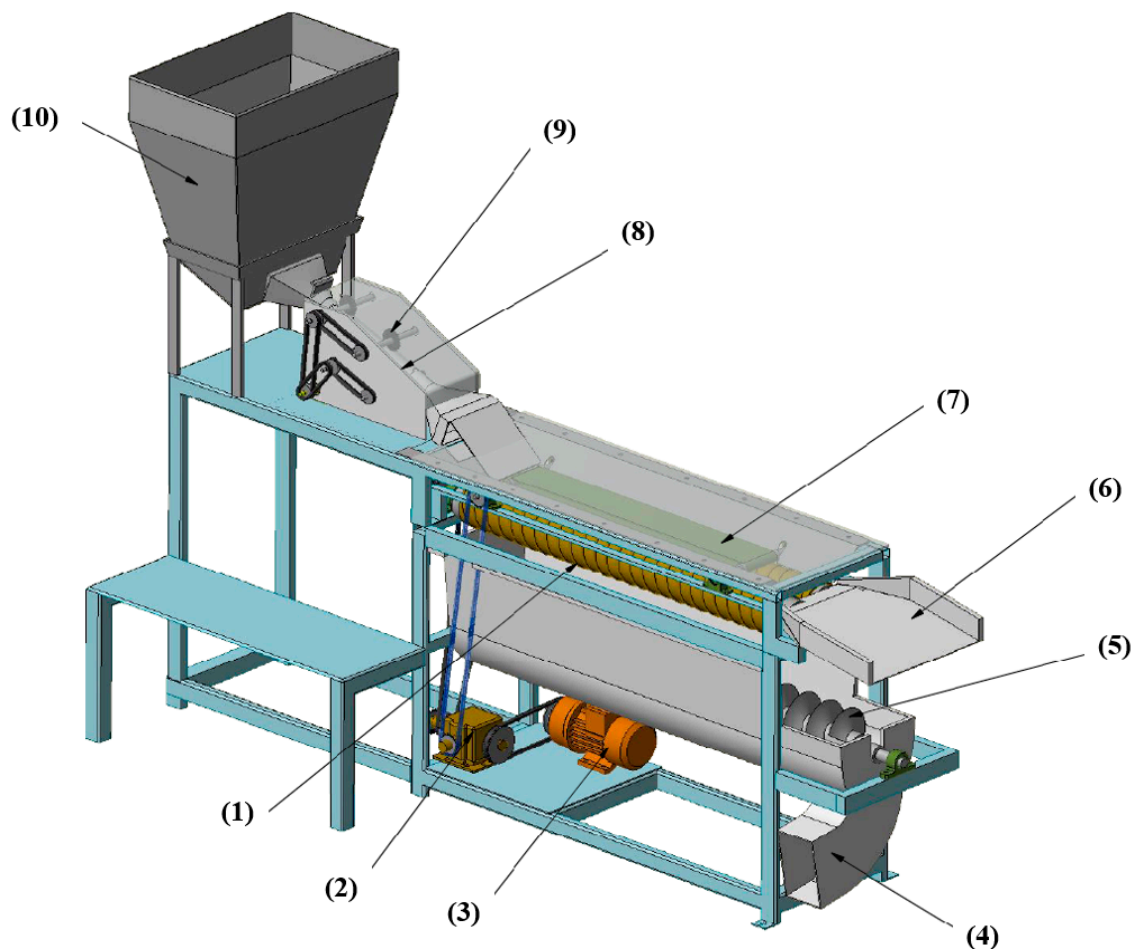


**Figure 11.** Assembly of different parts by Autodesk Inventor: (1) rollers; (2) gear box, (3) engine; (4) collection of peels; (5) spiral groove; (6) conveyor of peeled fruits; (7) pressing belt; (8) sorting conveyor; (9) blade; (10) hopper.

In short, various optimizations from both physical and mechanical points of view were investigated for obtaining properly working parameters of the peeling machine developed in this study. Especially, a pressing belt working under a pressure of 13.5 N and a speed of 140 mm/s was adopted. The belt length and width were also selected in an appropriate way taking into account the motion of the fruit along the length of the rollers. Such a pressing belt restricts the vertical motion of the fruit, so a better peeling rate and a lower pulp damage rate are obtained. Moreover, the gap between two rollers as well as their dimensions were carefully selected in function of mechanical and physical properties of the considered lychee fruits. In addition, spiral grooves along the axial direction of the rollers were created for better fruit guidance. An effective peeling machine such as this could help lychee manufacturers enhance their production chain, save time, and reduce damage.

#### 4. Conclusions and Outlook

This paper discusses the analytical development of a lychee peeling machine, combining the principles of friction and shearing. The main working part of the machine consists of two rubber-covered rollers and a pressing belt. This hybrid design was selected in order to reduce loss of pulp, juice, breakage, and flesh damage, compared to a peeling machine using pure friction. The mechanical properties of Thieu lychees were measured experimentally at the Strength of Materials Laboratory, Faculty of Engineering, Vietnam National University of Agriculture. The coefficient of static friction and critical peeling force of lychee fruits were determined as 0.90 and 10.5 N, respectively. In addition, the following physical characteristics of the fruits were also measured: size, shape, and mass density.

This information served as the basis for the design and analytical identification of optimal operational parameters. The results showed that, in order to separate the peel from the pulp of lychee fruits, the two rollers rotate in opposite directions at an optimal rotation speed of 159 RPM. The pressing belt, parallel to the rollers, is responsible for maintaining a minimum pressure of  $H = 13.5$  N on the fruits and transporting the lychees along the axial direction of the rollers with a velocity of  $V_{fruit} = 140$  mm/s. Using this design principle, the machine was able to work continuously with an expected throughput  $q = 100$  kg/h. In order to increase the throughput, it is possible to use multiple pairs of rollers and pressing belts together. Parametric studies showed that the roller length, diameter, and gap size between the rollers greatly affected the working capacity and quality of the machine. The roller needed to be long enough to allow sufficient time for peeling ( $L_{opt} = 900$  mm). The diameter of the rollers had to be large enough to create frictional torque for peeling ( $D_{opt} = 100$  mm). The gap size had to be large enough to allow the peel to pass through without becoming trapped and small enough to clamp and pull the peel downward ( $\delta_{opt} = 4$  mm).

However, several hypotheses have been made—the shape of the fruits was modeled as a sphere, and standard deviation in fruits' physical characteristics have not been taken into account. A prototype of the machine is currently fabricated and assembled for performing peeling task on actual lychee fruits in order to validate the chosen parameters. In addition, the expected throughput, peeling rate, pulp loss (based on calculation), and flesh quality (based on observation) are relevant parameters that could be used to quantify the validation of the machine. In further research, it would be of benefit to investigate rollers with differential rotation speed in order to deal with the non-spherical shape of lychees. On the other hand, numerical simulations such as Discrete Element Modelling coupled with Finite Element Analysis could be a potential candidate for tracking quickly what actually happen inside the main peeling part in terms of interaction forces taking into account irregular shapes of fruit. Finally, the methodology of modelling the peeling machine based on experimental data could pave the way for greater mechanization in many other post-harvesting problems, especially in developing countries.

**Author Contributions:** Conceptualization, L.M.L.; Data curation, T.C.N.; Formal analysis, T.C.N.; Funding acquisition, T.-T.L.; Investigation, T.C.N.; Methodology, L.M.L.; Project administration, B.T.P. and T.-T.L.; Resources, H.-B.L.; Software, H.-B.L.; Supervision, L.M.L.; Validation, V.M.L.; Visualization, B.T.P. and V.M. L.; Writing—original draft, H.-B.L., V.M.L., and T.-T.L.; Writing—review & editing, B.T.P.

**Funding:** This research received no external funding.

**Acknowledgments:** The authors gratefully acknowledge Vietnam National University of Agriculture for supporting this research.

**Conflicts of Interest:** The authors declare no conflict of interest.

## Abbreviations

Designation	Description	SI Unit
D	Roller diameter	mm
$D_{opt}$	Optimal roller diameter	mm
F	Force exerted on the arm	N
$F_{cr}$	Critical peeling force	N
$F_{fr}$	Friction force between fruit and roller	N
$F_{frb}$	Friction force between fruit and pressing belt	N
$F_{fr1}$	Friction force exerted on fruit by roller N°1	N
$F_{fr2}$	Friction force exerted on fruit by roller N°2	N

Designation	Description	SI Unit
$F_{sp}$	Force exerted on fruit by spring	N
H	Belt pressure	N
L	Roller length	mm
$L_{opt}$	Optimal roller length	mm
$L_{wl}$	Minimum working length of rollers	mm
N	Force exerted on fruit by roller	N
$N_1$	Radial force exerted on fruit by roller N°1	N
$N_2$	Radial force exerted on fruit by roller N°2	N
O	Center of gravity of fruit	-
$O_i, (i = 1, 2)$	Center of roller circular section	-
$P_1$	Tangential force exerted on fruit by roller N°1	N
$P_2$	Tangential force exerted on fruit by roller N°2	N
Q	Average fruit weight	kg
R	Roller radius	mm
S	Pitch of spiral groove	mm
$V_b$	Belt velocity	mm/s
$V_{fruit}$	Fruit velocity	mm/s
$V_{spr}$	Spiral velocity	mm/s
$Z_{fruit}$	Average number of fruits weighted 1 kg	-
a	Distance between two consecutive fruits along the roller axis	mm
d	Average fruit diameter	mm
f	Friction coefficient between fruit and roller	-
k	Spring stiffness	N/m
l	Level arm (moment arm)	mm
$n_r$	Number of fruit rounds	-
q	Expected throughput	kg/h
$\alpha$	Angle between $N_1$ (or $N_2$ ) and the horizontal	
$\beta$	Coefficient of distance between two consecutive fruits	-
$\gamma$	Coefficient of sliding of fruits	-
$\lambda$	Spring deformed length	mm
$\mu$	Coefficient of static friction	-
$\omega_1$	Rotation speed of roller N°1	RPM
$\omega_2$	Rotation speed of roller N°2	RPM
$\omega$	Rotation speed of roller	RPM
$\delta$	Gap size between two rollers	mm
$\delta_{opt}$	Optimal gap size	mm

## References

1. Caballero, B.; Trugo, L.; Finglas, P.M. *Encyclopedia of Food Science and Nutrition*; Academic Press: Cambridge, MA, USA, 2003; ISBN 978-0-12-227055-0.
2. Menzel, C.M.; Simpson, D.R. Lychee nutrition: A review. *Sci. Hortic.* **1987**, *31*, 195–224. [[CrossRef](#)]
3. Wang, C.; Zou, X.; Tang, Y.; Luo, L.; Feng, W. Localisation of litchi in an unstructured environment using binocular stereo vision. *Biosyst. Eng.* **2016**, *145*, 39–51. [[CrossRef](#)]
4. Vandever, M.L. Demand for area crop insurance among litchi producers in northern Vietnam. *Agric. Econ.* **2001**, *26*, 173–184. [[CrossRef](#)]
5. Tran, D.T.; Hertog, M.; Nicolai, B.M. Hierarchical response surface methodology for optimization of postharvest treatments to maintain quality of litchi cv. 'Thieu' during cold storage. *Postharvest Biol. Technol.* **2016**, *117*, 94–101. [[CrossRef](#)]
6. Qiao, F.; Huang, L.; Xia, W. A study on microwave vacuum dried re-structured lychee (*Litchi chinensis* Sonn.) mixed with purple sweet potato (*Ipomoea batatas*) snacks. *Food Bioprod. Process.* **2012**, *90*, 653–658. [[CrossRef](#)]
7. Kosseva, M.; Joshi, V.K.; Panesar, P.S. *Science and Technology of Fruit Wine Production*; Academic Press: Cambridge, MA, USA, 2016; ISBN 978-0-12-801034-1.
8. Holcroft, D.M.; Mitcham, E.J. Postharvest physiology and handling of litchi (*Litchi chinensis* Sonn.). *Postharvest Biol. Technol.* **1996**, *9*, 265–281. [[CrossRef](#)]
9. Xiong, J.; Lin, R.; Liu, Z.; He, Z.; Tang, L.; Yang, Z.; Zou, X. The recognition of litchi clusters and the calculation of picking point in a nocturnal natural environment. *Biosyst. Eng.* **2018**, *166*, 44–57. [[CrossRef](#)]
10. Batten, D.J. Maturity criteria for litchis (lychees). *Food Qual. Prefer.* **1989**, *1*, 149–155. [[CrossRef](#)]
11. Wang, W.; Lu, H.; Zhang, S.; Yang, Z. Damage caused by multiple impacts of litchi fruits during vibration harvesting. *Comput. Electron. Agric.* **2019**, *162*, 732–738. [[CrossRef](#)]
12. Moustier, P.; Tam, P.T.G.; Anh, D.T.; Binh, V.T.; Loc, N.T.T. The role of farmer organizations in supplying supermarkets with quality food in Vietnam. *Food Policy* **2010**, *35*, 69–78. [[CrossRef](#)]
13. He, Z.-L.; Xiong, J.-T.; Lin, R.; Zou, X.; Tang, L.-Y.; Yang, Z.-G.; Liu, Z.; Song, G. A method of green litchi recognition in natural environment based on improved LDA classifier. *Comput. Electron. Agric.* **2017**, *140*, 159–167. [[CrossRef](#)]
14. Thompson, A.K. Postharvest Technology of Fruits and Vegetables. In *Fruit and Vegetables*; John Wiley & Sons: Hoboken, NJ, USA, 2007; pp. 115–369. ISBN 978-0-470-75106-0.
15. Bochtis, D.D.; Sørensen, C.G.C.; Busato, P. Advances in agricultural machinery management: A review. *Biosyst. Eng.* **2014**, *126*, 69–81. [[CrossRef](#)]
16. Li, X.; Pan, Z.; Atungulu, G.G.; Zheng, X.; Wood, D.; Delwiche, M.; McHugh, T.H. Peeling of tomatoes using novel infrared radiation heating technology. *Innov. Food Sci. Emerg. Technol.* **2014**, *21*, 123–130. [[CrossRef](#)]
17. Siddiq, M. *Tropical and Subtropical Fruits: Postharvest Physiology, Processing and Packaging*; John Wiley & Sons: Hoboken, NJ, USA, 2012; ISBN 978-1-118-32411-0.
18. Nguyen, X.T.; Bernhardt, G. Influences of Concave Length and Feeding Angle on Separation Capacity in the Multi-cylinder Threshing System. *Landtechnik* **2008**, *63*, 276–277.
19. Manjunatha, M.; Samuel, D.V.K.; Anurag, R.K.; Gaikwad, N. Development and performance evaluation of a garlic peeler. *J. Food. Sci. Technol.* **2014**, *51*, 3083–3093. [[CrossRef](#)]
20. Chen, H.; Xu, X.; Yin, Y.; Pan, H.; Bao, X.; Li, S.; Xu, Q. Experimental study on mechanical properties and peel separation characteristics of citrus reticulate blanco with peel clamped moving. *Nongye Gongcheng Xuebao* **2017**, *33*, 25–31.
21. Pan, H.; Wang, Z.; Chen, H.; Liu, J.; Tong, Y.; Shi, X. Design and experiment on dual rollers peeling machine for satsuma mandarin. *Nongye Gongcheng Xuebao* **2015**, *31*, 239–245.
22. Vidyarthi, S.K.; El Mashad, H.M.; Khir, R.; Zhang, R.; Tiwari, R.; Pan, Z. Evaluation of selected electric infrared emitters for tomato peeling. *Biosyst. Eng.* **2019**, *184*, 90–100. [[CrossRef](#)]
23. Jimoh, M.O.; Olukunle, O.J. An Automated Cassava Peeling System for the Enhancement of Food Security in Nigeria. *Niger. Food J.* **2012**, *30*, 73–79. [[CrossRef](#)]
24. Purbey, S.; Kumar, K.K. *Tools and Machinery for development of Litchi*; Tools and machinery for Development of Horticulture: Kerala, India, 2009.

25. Vishwakarma, R.; Nambi, E.; Gupta, R.K. Litchi Fruit Peeling Machine. Available online: <https://icar.org.in/content/directorate-knowledge-management-agriculture> (accessed on 1 September 2019).
26. CN103445277A-Lychee Branch Removal Machine-Google Patents. Available online: <https://patents.google.com/patent/CN103445277A/en?inventor=%E5%86%AF%E5%8B%8B%E5%81%A5> (accessed on 1 September 2019).
27. Henan Hiwant International Co., Ltd. Haihuang Industrial Zone, middle section of Anlin rd, Anyang, Henan, China. Available online: <http://www.hifruitmachine.com/Fruit%20Processing%20Products/lychee-litchi-lichee-longan-rambutan-peeling-machine/> (accessed on 1 September 2019).
28. Menzel, C.M.; Simpson, D.R. Growth, flowering and yield of lychee cultivars. *Sci. Hort.* **1992**, *49*, 243–254. [[CrossRef](#)]
29. Xiong, J.; He, Z.; Lin, R.; Liu, Z.; Bu, R.; Yang, Z.; Peng, H.; Zou, X. Visual positioning technology of picking robots for dynamic litchi clusters with disturbance. *Comput. Electron. Agric.* **2018**, *151*, 226–237. [[CrossRef](#)]
30. Qing, Y.; Li, C.; Cao, Y.; Zhang, Z.; Cheng, H. Test and analyse on macromechanic parameters of longan. *Nongye Jixie Xuebao* **2010**, *41*, 125–134.
31. Wang, F.; Wang, C.; Yang, X. Mechanics characteristics and finite element analysis of watermelon. *Trans. Chin. Soc. Agric. Eng.* **2008**, *24*, 118–121.
32. Junwei, L.; Yunhai, M.; Jin, T.; Zichao, M.; Lidong, W.; Jiangtao, Y. Mechanical properties and microstructure of potato peels. *Int. J. Food Prop.* **2018**, *21*, 1395–1413. [[CrossRef](#)]
33. Kunpeng, T.; Shen, C.; Xianwang, L.; Huang, J.; Qiaomin, C.; Bin, Z. Mechanical properties and compression damage simulation by finite element for kiwifruit. *Int. Agric. Eng. J.* **2017**, *26*, 193–203.
34. Williams, H.A.M.; Jones, M.H.; Nejati, M.; Seabright, M.J.; Bell, J.; Penhall, N.D.; Barnett, J.J.; Duke, M.D.; Scarfe, A.J.; Ahn, H.S.; et al. Robotic kiwifruit harvesting using machine vision, convolutional neural networks, and robotic arms. *Biosyst. Eng.* **2019**, *181*, 140–156. [[CrossRef](#)]
35. Singh, K.K.; Boreddy, S. Postharvest physico-mechanical properties of orange peel and fruit. *J. Food Eng.* **2006**, *73*, 112–120. [[CrossRef](#)]
36. Chen, Y.; Li, J.; Wang, J.; Jiang, Z.; Zou, X.; Liu, W. Test of Mechanical Parameters for Litchi and Analysis for Its Difference. *DEStech Trans. Mater. Sci. Eng.* **2017**. [[CrossRef](#)]
37. Chen, Y.; Cai, W.; Zou, X.; Xiang, H. Extrusion mechanical properties of fresh litchi. *Nongye Gongcheng Xuebao* **2011**, *27*, 360–364.
38. Chen, Y.; Cai, W.; Zou, X.; Xiang, H.; Liu, T.; Xu, F. Mechanical properties test and finite element analysis for litchi. *Nongye Gongcheng Xuebao* **2011**, *27*, 358–363.
39. Chen, Y.; Cai, W.; Xiang, H.; Zou, X.; Tan, J.; Lin, G. Mechanical properties of litchi stem for harvesting robots. *Nongye Gongcheng Xuebao* **2012**, *28*, 53–58.
40. Wang, W.; Yang, Z.; Lu, H.; Fu, H. Mechanical damage caused by fruit-to-fruit impact of litchis. *IFAC-PapersOnLine* **2018**, *51*, 532–535. [[CrossRef](#)]
41. Xiong, J.; Lin, R.; Bu, R.; Liu, Z.; Yang, Z.; Yu, L. A Micro-Damage Detection Method of Litchi Fruit Using Hyperspectral Imaging Technology. *Sensors* **2018**, *18*, 700. [[CrossRef](#)] [[PubMed](#)]
42. Yousefi, S.; Farsi, H.; Kheiralipour, K. Drop test of pear fruit: Experimental measurement and finite element modelling. *Biosyst. Eng.* **2016**, *147*, 17–25. [[CrossRef](#)]
43. Ghodki, B.M.; Patel, M.; Namdeo, R.; Carpenter, G. Calibration of discrete element model parameters: Soybeans. *Comput. Part. Mech.* **2019**, *6*, 3–10. [[CrossRef](#)]
44. Ly, H.-B.; Pham, B.T.; Dao, D.V.; Le, V.M.; Le, L.M.; Le, T.-T. Improvement of ANFIS Model for Prediction of Compressive Strength of Manufactured Sand Concrete. *Appl. Sci.* **2019**, *9*, 3841. [[CrossRef](#)]
45. Mezhericher, M.; Brosh, T.; Levy, A. Modeling of Particle Pneumatic Conveying Using DEM and DPM Methods. *Part. Sci. Technol.* **2011**, *29*, 197–208. [[CrossRef](#)]
46. Autodesk Inventor Version 22.0; Autodesk: San Rafael, CA, USA, 2018.

